Study of Crosslinking Copolymerization and its Fractal Behavior of Styrene-Divinylbenzene

JU ZUO,[1,2] DEHAI LIANG,[1] SHAOFENG RAN,[1] TIANHONG CHEN,[1] AIZHEN NIU,[1] BINGLIN HE[2]

[1] Department of Chemistry, Nankai University, Tianjin 300071, People's Republic of China

[2] The State Key Laboratory of Functional Polymeric Materials for Adsorption and Separation, Nankai University, Tianjin 300071, People's Republic of China

Received 21 January 1997; accepted 9 August 1997

ABSTRACT: The crosslinking copolymerization of styrene-divinylbenzene (DVB) with 6% (w/w) DVB was investigated quantitatively by liquid chromatography (LC), viscosity, GPC, and static and dynamic laser light. Through these experiments, reaction order, mechanism, and evolution of molecular weight, size, polydispersity, and branching of the copolymer chains during the gelation were measured. The critical exponents γ, β, δ, τ, and ν_p of the gelation were calculated. Furthermore, fractal behavior of the copolymer was evidenced firmly; the progression of fractal dimensions of these species following the gelation were also obtained using the dependence of intensity scattered on angles by synchrotron small angle X-ray scattering. A methodology for characterization of gelation forming network polymer is provided objectively. © 1998 John Wiley & Sons, Inc. J Appl Polym Sci 68: 363–371, 1998

Key words: styrene-divinylbenzene; crosslinking copolymerization; scaling; critical exponent; fractal

INTRODUCTION

Many theories have been developed to describe the molecular processes involved in gel formation during various polymerizations since Carothers[1] defined a gel as a three dimensional molecule with an infinitely large molecular weight. Pioneering work was done by Flory/Stockmayer.[2–4] Their classical gelation theory established the framework for further developments. Most statistical theories, which differ in mathematical language, are outstanding examples. However, these statistical models, which involved complex mathematics, require random formation of crosslink points on accumulated polymer chains at all levels of monomer conversion during polymerization and thus inherently treat gelation as a process in thermodynamic equilibrium. But the reactions involved in free-radical polymerization are, in fact, kinetically controlled. The development of chain properties depends strongly on the reaction path. In this respect, the statistical models are not realistic.[5,6] Much more effort has been made to improve these.[6,7]

Another type is called percolation theory.[8] Though the percolation theory may possess potential universality, it is still too immature to describe the course of network formation and its predictions are just qualitatively acceptable. At present, it is still considered controversial and unclear which theory is more suitable for polymeric gelation.

An important field where fractals are observed is that of far-from-equilibrium growth phenomena. Examples of such processes include the aggregation of similar particles or clusters which

Correspondence to: Ju Zuo.

Contract grant sponsor: The National Nature Science Foundation of China; contract grant sponsor: BEPC NL.

Journal of Applied Polymer Science, Vol. 68, 363–371 (1998)
 CCC 0021-8995/98/030363-09

stick together and the gelation of many growing clusters which crosslink, forming a network. These represent the very important classes of growth phenomena producing complicated geometrical objects, and are called fractal growth phenomena because of creating fractals.[9]

As a result, it is reasonable to study crosslinking copolymerization of styrene-DVB, which should belong to fractal growth phenomena. The reasons are at least as follows: (1) simpler mathematics, which is important for a general chemist; (2) it is the more appropriate way to understand the properties of the crosslinking radical copolymerization.

The objects of this article are both to investigate systematically and quantitatively the process of the radical crosslinking copolymerization of styrene-DVB and to evidence their fractal behavior, which hasn't been probed experimentally yet so far, mainly by static dynamic laser scattering and small angle X-ray scattering. Furthermore, using above experimental results, we also wish to gain more information about the distribution of macromolecular chains branched, and finally a novel fractal geometry methodology for studying this kind of gelation reaction is provided objectively.

EXPERIMENTAL

Sample Preparation[10]

The samples were synthesized by simple radical crosslinking copolymerization in bulk at 60 $\pm$ 0.1°C. We used monomer mixtures of styrene and technical DVB (57.52% DVB was a mixture of DVB isomers, the remainder was mainly ethylstyrene) as reactant. Prior to use styrene was dried with CaH_2, distilled under vacuum. DVB was deinhibited by 10% NaOH aqueous saturated with NaCl, then washed to neutral, also dried over CaH_2. After treating, both were kept in a refrigerator temporarily. Styrene, DVB, and benzoyl peroxide (BPO) were mixed at the ratio of 94 : 6 : 0.1 or 0.05 by weight, which were designated in the following as P_1 and P_2, respectively. The initial reactant was divided into about 20 100-mL ampules and about the same number 10-mL ampules, then sealed immediately after degassing and filling by nitrogen. The reactant in bigger or smaller ampules was for sampling or for LC, respectively. At desired time intervals the ampule was taken out of a thermostatic bath and quenched by liquid nitrogen for terminating reaction immediately. The reactant in the bigger ampule was precipitated by methanol and dried in vacuum oven at about 50°C until constant weight for following experiments. Solvent CCl_4 with internal calibrator C_{14} was added into the smaller ampules to determine conversions of the monomers by LC. The conversions for sample P_1 were reported in Table I. Those of P_2 were not measured.

Table I The Conversions of Monomers for Sample P_1 Following the Gelation

Time (h)	St %	m-DVB %	P-DVB %
2	0.079	7.68	8.22
3	0.772	9.51	10.25
4	3.68	13.87	14.64
5.7 (t_g)	4.67	15.30	20.12
6.5	4.90	15.80	20.63
8	10.63	24.46	31.29
10	11.85	29.63	40.90
12	21.33	41.82	55.90
15	34.16	62.41	81.00
18	56.34	83.21	98.27
20	71.03	92.77	100
25	86.84	100	
30	92.39		
35	92.94		
46.5	93.27		
48	93.68		

The same initial reactant (10 mL) was also put into a special viscometer, in which the same copolymerization was taken place, for tracing the change of the viscosity of the reactant in order to detect the gelation time (t_g). Prior to reaction the initial reactant in the viscometer underwent the same treatment as mentioned above and then its viscosity was measured during the gelation at 60 $\pm$ 0.2°C under protection of nitrogen.

LC Measurement

The conversions in Table I were measured by Shimadzu-9A, Japan.

GPC Measurement

The molecular weights of weight average and number average of the samples for the pre-gel point were measured by a Waters GPC 244, USA. The calibration curve was made with linear polystyrene.

Viscosity Measurement

The intrinsic viscosities $[\eta]$ of toluene solution of samples for pre-gelation point were measured by a Ubbelohde viscometer at 25 ± 0.1°C.

Static and Dynamic Light Scattering Measurement

A spectra-physics Ar^+ laser (λ = 514.5 nm) was used in conjunction with a 64-channel clipped digital autocorrelator model 1096 (Langley-Ford Instruments Corporation) for measuring both static and dynamic measurement. Scattering angles were varied from 30° to 135°. The experiment was performed at 25 ± 0.1°C.

The static intensity data were routinely processed by using a Zimm plot to yield the weight-average molecular weight (M_w), the mean-square radius of gyration (R_g) and the second virial coefficient (A_2).

For dynamic light scattering, cumulants analysis was used to calculate the average decay rate Γ and variance POLY. of correlation function for each measurement. The variance is a measure of the width of distribution of decay rate and is given by

$$\mathrm{POLY} = \mu^2/\Gamma \qquad (1)$$

where μ^2 is the second moment of the distribution. The translational diffusion coefficient D_T and the hydrodynamic radius R_h were obtained from the average decay rate Γ and Stokes–Einstein formula, respectively, according to

$$D_T = \Gamma/q^2 \qquad (2)$$

and

$$R_h = K_bT/6\pi\eta D_T \qquad (3)$$

Where the scattering vector $q = 4\pi n/\lambda \sin \theta/2$ with θ, λ, K_b, T, η and n being the scattering angle, the incident wavelength in vacuum, Boltzmann constant, absolute temperature, solvent viscosity, and solvent refractive index, respectively.

Small Angle X-ray Scattering Measurement

The small angle X-ray scattering experiments were carried out at Beijing Synchrotron Radiation Laboratory (BSRL) of the Beijing Electron Positron Collider National Laboratory (BEPC NL) in Beijing China. λ = 0.54 nm, measuring range 1.75 $\times 10^{-2} < q < 1.18$ nm^{-1}. The size of the sample string is 25 mm × 6 mm, thickness 0.6 mm (ca). The distance from the sample to the detector is 1.4 m. The scattered intensity data were processed by using fractal theory in order to determine whether or not there is fractal behavior during this copolymerization.

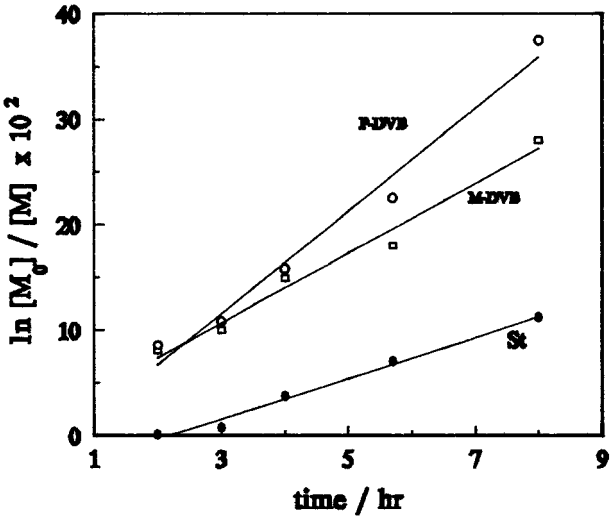

Figure 1 The plots of $\ln[M_0]/[M]$ versus reaction time t for sample P_1.

RESULTS AND DISCUSSION

Crosslinking Copolymerization

Figure 1 shows the plot of $\ln[M_0]/[M]$ as a function of time in the experimental period. Here M_0, M are the concentrations of monomers at the beginning and the sampling time t, respectively. So it is observed that the conversions of all three monomer species during the crosslinking copolymerization of styrene-DVB obey first-order laws within experimental accuracy. This means that if one of the monomers is converted into polymer according to a first-order law, the same should be true for the second monomer even though the DVB is high, 6%, instead of 2%,[11] of the total concentration of styrene-DVB. The evolution of M_w for sample P_1 during the copolymerization of styrene-DVB is showed in Figure 2. It is obvious that the M_w increase pronouncedly following the copolymerization and give rise to divergence near t_g from both data of light scattering and GPC. According to the theory of Flory/Stockmayer, the increasing of the molecular weight of sol with time during gelation has the relation

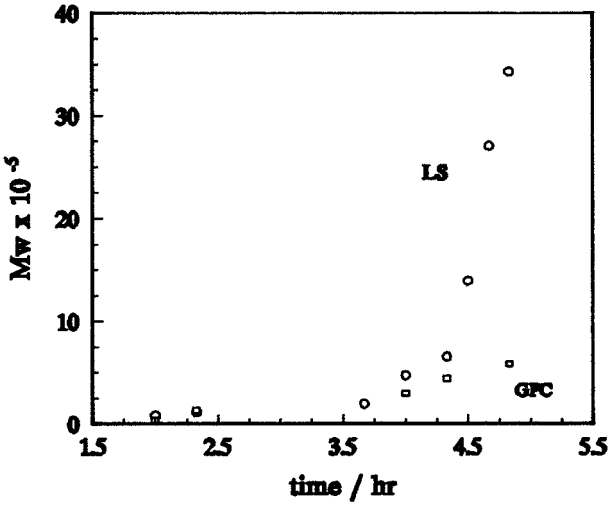

Figure 2 The evolution of molecular weight M_w for sample P_1 following the copolymerization.

$$M_w \propto (1 - t/t_g)^{-\gamma} \quad (4)$$

here $\gamma = 1.94$ from our data. The value is some higher than 1.76 of sol colloid.[12] It implies that the divergence of the gelation present is stronger than that of standard percolation model.

The sizes of these species during the gelation, including R_g and R_h, also increase and diverge markedly near t_g. R_g, however, develops much faster than R_h (Fig. 3).

The ratio δ ($=R_g/R_h$) is a parameter influenced by density and polydispersity. Although the two factors all will make δ value increase, the effect of polydispersity is more efficient. Here δ values

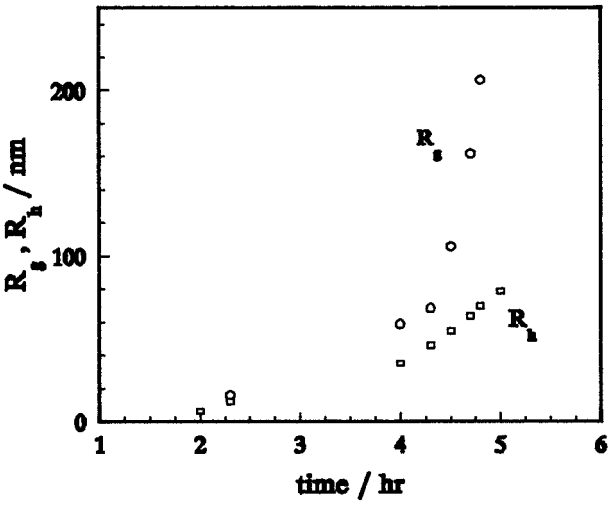

Figure 3 The evolution of molecular size for sample P_1 following the copolymerization.

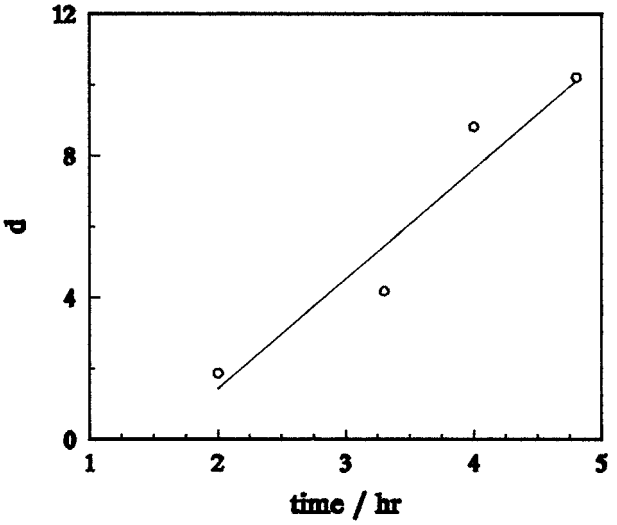

Figure 4 The change of the parameter d during the copolymerization of sample P_1.

go up monotonously and finally reach much higher value 6 (ca), which is 1.4 ~ 2.0 for linear polystyrene in solution[13] and a little higher for branched polystyrene than the linear one. Therefore, obviously, much higher δ values imply that the polydispersities of these species are mainly responsible for that and also its influence increase more pronouncedly than branching following the gelation.

Figure 4 shows that the parameters $d = (M_w/M_n)$ from GPC go up outstandingly following the gelation. It agrees well with experimental results of the δ values. Another evidence present for polydispersity is variance μ^2/Γ in dynamic light scattering. It is a measure of relative width of the Z-average diffusion coefficient, dimensionless μ^2 is the second moment. If a sample is monodisperse, its variance is about 0.02, a typical lower limit, but the variances of these species here are all around 0.2. Thus it tells us that this system is rather polydisperse.

Furthermore, although the effect of branching is not so obvious as mentioned above, it does exist during the gelation. The branching parameter

$$G = ([\eta]_b)/([\eta]_1) \quad (5)$$

reflects the degree of branching, which is measured under the same molecular weights for linear and branched samples. $[\eta]_b$ and $[\eta]_1$ are intrinsic viscosities of branched and linear samples, respectively. Branching will result in the decrease

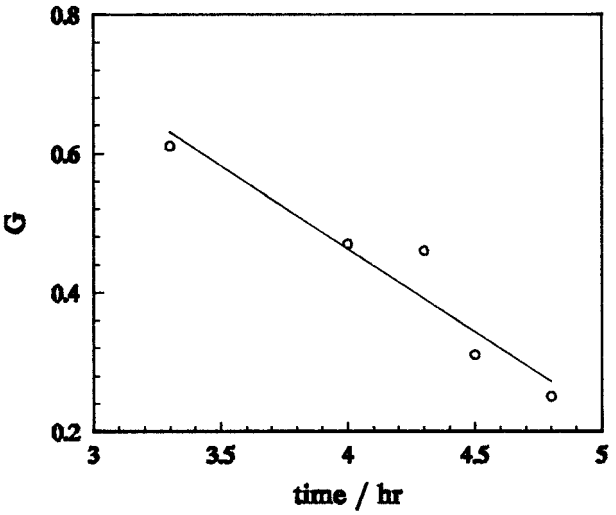

Figure 5 The plot of parameter G against reaction time t for sample P_1.

of $[\eta]_b$. As a result, G values should decrease following the gelation. Figure 5 shows us the rule.

In Figure 2, that the M_w from LS is much higher than from GPC is another evidence for branching. The reason is that at same elution volume, M_w branched is larger than linear. Hence, when linear polystyrene is used as a standard sample for calibration curve, the M_w of the sample branched from GPC must be lower than from LS. And the bigger the difference, the more the branching.

So far, reaction order, mechanism, and the evolution of molecular weight, size, polydispersity, and branching of copolymers during the crosslinking copolymerization of styrene with 6% DVB by weight have been represented quantitatively, which is a significant event for understanding and controlling sol-gel transition reaction, and especially necessary for exploring its fractal behavior in the following.

Scaling and Critical Exponents

As is well known, gelation is a particular critical phenomenon, so certain quantities can be used to describe the system, which are independent of the actual materials and of the details of the models employed. These are called universal quantities. Examples of universal quantities are the critical exponents obtained from scaling relationships between one physical property of a system and another near the transition point, that is, the M_w and the distance from t_g as measured by the extent of reaction.

In polydisperse samples,[14] the scaling of any average quantities with another will in general depend on which average is involved and on the distribution of molecular weights. For $P > P_c$, we have the following relation:

$$G \sim |P - P_c|^{\beta} \tag{6}$$

where β is the critical exponent relating extent of reaction P (P_c, extent of react at t_g) to the gel fraction G. For $P < P_c$, the weight-average molecular weight must diverge as

$$M_w \sim |\mathrm{P} - \mathrm{P}_c|^{-\gamma} \tag{7}$$

Both β and γ are critical exponents.

Returning to the form of the distribution function, the distribution of molecular weights for gelling sample is given by

$$P(M, P) = M^{-\tau} f(M/M_{\mathrm{char}}) \tag{8}$$

where f is a cutoff function, τ is a critical exponent, and M_{char} is the characteristic molecular weight for a sample at a particular extent of reaction. This characteristic molecular weight diverges near t_g, defining another critical exponent σ:

$$M_{\mathrm{char}} \sim |P - P_c|^{1/\sigma} \tag{9}$$

and there are two relations:

$$\beta = (\tau - 2)/\sigma \tag{10}$$

$$\gamma = (3 - \tau)/\sigma \tag{11}$$

It is clear from equations 10 and 11 that of the four critical exponents defined so far, only two are independent.

In addition, the scaling relationship between size and molecular weight for a diluted polydisperse sample should have the following relation:

$$\langle R_g^2 \rangle_z \sim M_w^{2\nu_e} \tag{12}$$

and

$$\nu_e = \nu^B/(3 - \tau) \tag{13}$$

where ν^B is the scaling exponent between size and weight for randomly branched polymer of a single chain. The exponent ν_e contains information on both the solvent quality through the exponent ν^B and the distribution of molecular weights through

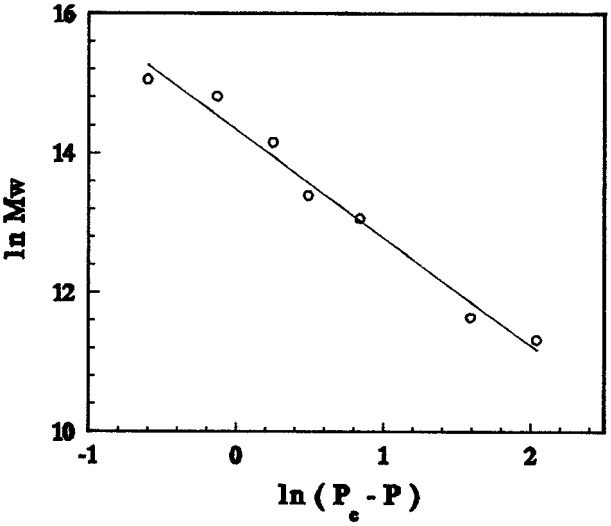

Figure 6 The ln–ln plot of M_w against $(P_c - P)$ for sample P_1.

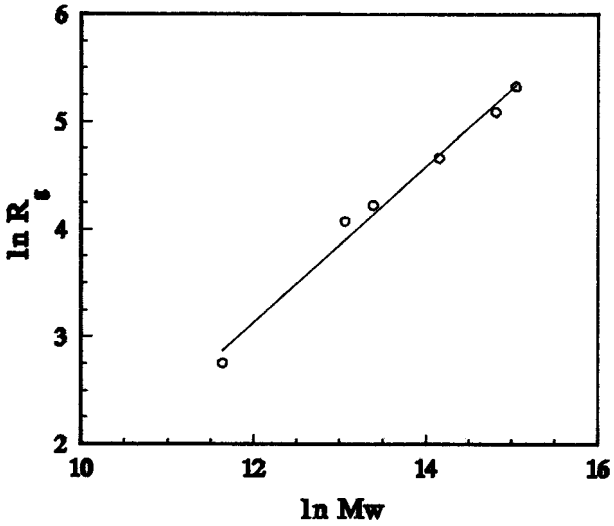

Figure 7 The ln–ln plot of R_g against M_w for sample P_1.

the critical exponent τ. To separate the two factors from each other, the results from intrinsic viscosity must be used. The relationship between the average quantities observable in experiments on a diluted system is as follows:

$$[\eta] \sim M_w^{(3\nu^B-\tau+1)/(3-\tau)} \tag{14}$$

From eqs. (12–14), the values of the individual exponents, ν^B and τ can be obtained. Thus, from eqs. (7, 10, and 11), the critical exponents γ, β, and σ can also be given.

Furthermore, the ν_p is the gelation exponent, which is defined in the relationship between the characteristic length ξ in the system and the distance from t_g by

$$\xi \sim |P - P_c|^{-\nu_p} \tag{15}$$

Hyperscaling can be expressed as

$$d\nu_p = \gamma + 2\beta = (\tau - 1)/\sigma \tag{16}$$

which relates ν_p and dimensionality of space d to the two measured exponents.

Figure 6 is the ln–ln plot of M_w vs. $|P - P_c|$. From the linear relationship showed in Figure 6, γ is 1.66 by using eq. (7). Figure 7 is the plot of ln R_g against ln M_w and its slope, ν_e, is 0.616. Again, from plot of ln$[\eta]$ vs. ln M_w (Fig. 8), slope is 0.400. Then τ equals 2.10 by using both slopes and eqs. (12–14). Thus, σ, β, and ν_p calculated by eqs. (10, 11, and 16) are 0.52, 0.31, and 0.76, respectively, Here $d = 3$ is chosen. These critical exponents are summarized and compared in Table II. Consequentially, our experimental results are more close to the percolation theory. It is rather reasonable.

Fractal Behavior

From a geometrical point of view, species (clusters) obtained above also can be characterized quantitatively by their fractal dimension.

For a random structure from colloidal aggregation or gelation, there is no exact self-similarity.

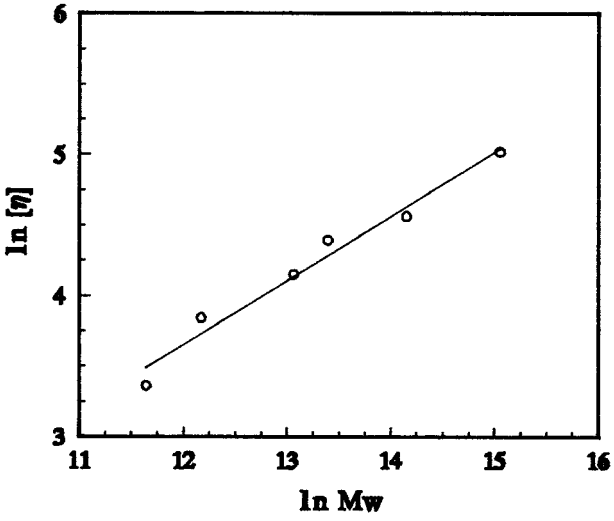

Figure 8 The ln–ln plot of $[\eta]$ against M_w for sample P_1.

Instead, we may have an average or statistical self-similarity. This means that the correlation function which describes the structure from fractal growth has a scale invariant (power law) form. It is also important to recognize that for statistically self-similar fractals found in nature, geometric scaling relationships are not valid for all length scales. For example, in the case of a colloidal aggregate consisting of particles with a radius r_0 and having an overall radius of R_0, the scale invariant form is correct only for length scales (l) in the range $r_0 < 1 < R_0$.[15]

For colloidal aggregates and other random fractals in real space, it is convenient to think of the fractal dimensionality in term of the scaling relationship between mass (M) and length (l)

$$M \sim l^{D_f} \tag{17}$$

The relationship of this type is frequently employed to measure the fractal dimensionality. D_f is the fractal dimension (Hausdorff dimension). For a polydisperse polymer, we approximate the expression to be $M_w \sim (\langle R_g^2 \rangle^{1/2})^D$.[16] Therefore, if the radius of gyration R_g is measured as a function of aggregate mass (M_w), then it is easy to get the fractal dimension D_f through the ln–ln plot of M_w against R_g (Fig. 9). The straight line shows existence of fractal dimensionality for our reaction system, and the slope is just fractal dimension. Here $D_f = 1.59$.

Furthermore, Figure 9 and D_f value not only reveal fractal behavior of this gelation but also mechanism. As is well known, if these clusters grow in three dimensions, D_f is around 2.0 predicted by reaction-limited cluster aggregation model (RLCA). And if growth of these clusters are in two dimensions, their D_f is 1.53 ± 0.01 or $1.59 + 0.01$ for mono- or poly-dispersity,[17] respectively. Surprisingly, the latter is fit well for our data and thus is responsible for a lower D_f (1.59) value, so this approach is powerful for knowledge

Table II Summary and Comparison of Critical Exponents for Sample P_1

Exponent	Percolation	Flory–Stockmayer	Exptl.
τ	2.20	2.5	2.10
γ	1.74	1	1.94
β	0.45	1	0.31
σ	0.46	0.5	0.52
ν_p	0.88	0.5	0.76

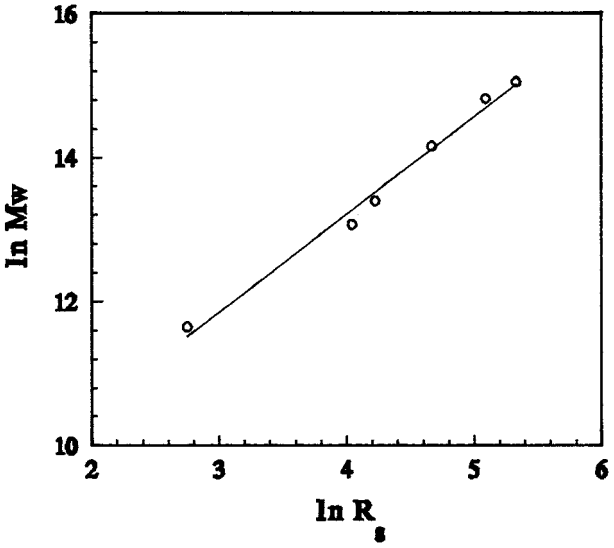

Figure 9 The ln–ln plot of M_w against R_g for sample P_1.

of chemical reaction. As to why two dimensions instead of three dimensions, it is easy to explain using a tip-model,[18,19] which consequently leads to a smaller fractal dimension of cluster. Here we may think an active center in copolymerization as a tip.

In addition, exponential growth of R_h with time is more evidence for RLCA.[20] In our case

$$R_h = 5.195 \exp(0.872\, t) \tag{18}$$

The RLCA mechanism, therefore, of the gelation present is confirmed again.

A straightforward way to detect fractality is to perform a resolution analysis,[21] that is, the study of variation of a measurable property when the yardstick size is changed. The scattering method is one among the main types for resolution analysis. In a scattering process, momentum transfer is measured and modules q of scattering vector $|q| = 4\pi/\lambda \sin \theta/2$ plays the role of the measuring yardstick to the probe fractal structure. The current study involves small angle scattering of X-ray where the higher q range is accessible. Basically, the static structure factor $s(q)$ is the Fourier transform of pair-correlation function and it has been shown that for monodisperse fractal cluster of dimension D_f, $s(q)$ will scale with q according to the power law $s(q) \sim q^{-D}$ for $qR_g \gg 1$. As scattered intensity $I(q)$ is proportion to $s(q)$, the measurement of scattered intensity (on a relative scale) provides in principle a simple way to determine D_f from scaling relation.

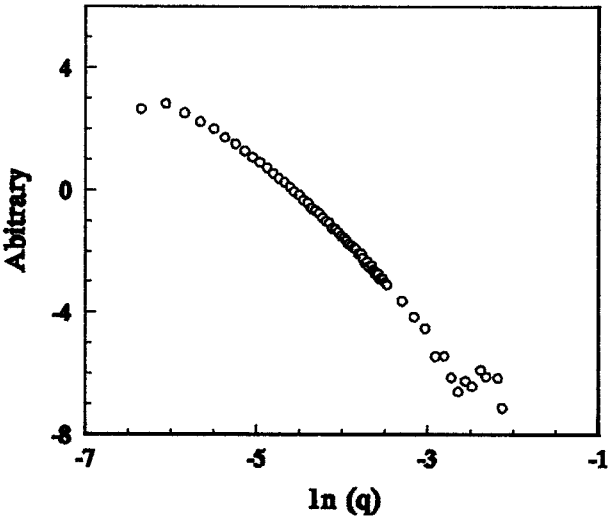

Figure 10 The ln–ln plot of $I(q)$ against q for sample P_2.

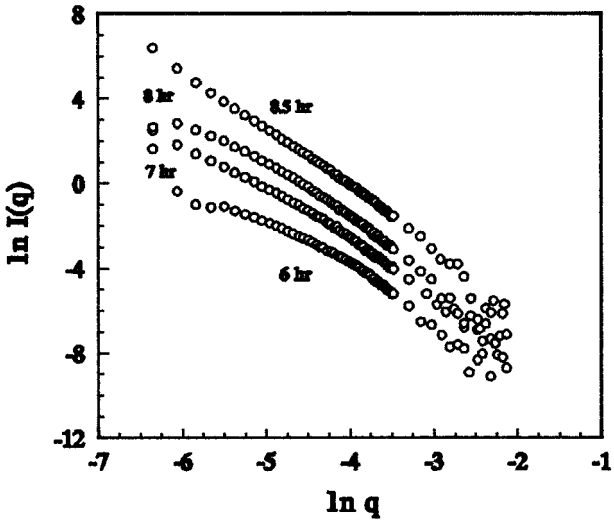

Figure 11 The ln–ln plots of $I(q)$ against q for sample P_2.

$$I(q) \sim q^{-\alpha} \tag{19}$$

From a monodisperse system, $|\alpha|$ is then usually identified with D_f in an interval

$$1/R_g < q < 1/a \tag{20}$$

defined by dimension of cluster R_g and constituent elementary particle a. Also for a polydisperse system, $|\alpha|$ may be identified approximately with D_f so long as time correlation functions still decay single-exponentially in dynamic light scattering, which is true for us. The approximate principle may be suitable to both solution or solid samples, which is for light scattering or X-ray scattering present, respectively.

In Figure 10, the ln–ln plot of $I(q)$ against q shows a rather well straight line in a certain q range. This result not only reveals real existence of fractal behavior during this gelation again by another way, but also probes fractal dimension $|D_f|$ using solid sample from slope.

According to Figure 11, the power-law fractal behavior covers a relatively shorter q-range at earlier stages of copolymer formation. As the copolymerization reaction progresses, the fractal power-law region in Figure 11 extends toward lower q values because of the increase of size R_g of branched molecular cluster. Near t_g (about 8.5 h), R_g becomes quite large and a substantial portion of the q range obeys the equation. At the same time, the slopes of these curves are increased. It means that the fractal dimension of copolymer increases gradually during the gelation.

Figure 12 shows the entire evolution process of fractal dimension during the crosslinking copolymerization of sample P_2, which includes the species in pre- and post-gelation point. This curve may be divided into three regions. Region 1 is characterized by rapid increase in the D_f value and K-range extends toward lower K values gradually. Growth and branching of copolymer chains in region 1 continue, so the structures and sizes of these chains become more and more complex and larger, respectively.

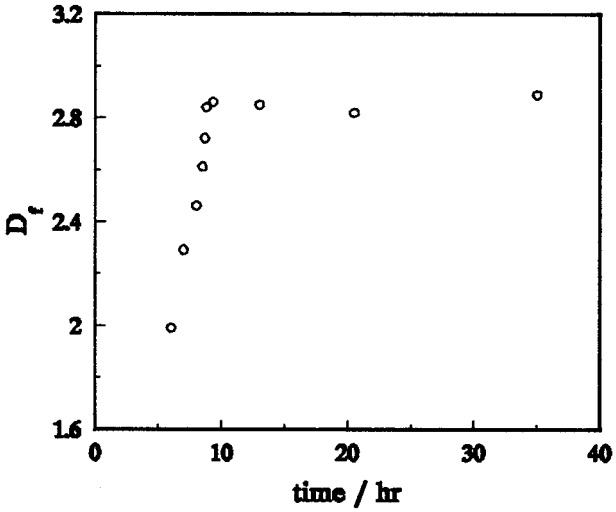

Figure 12 The evolution of fractal dimension D_f for sample P_2.

At the end of region 1, the gelation time is reached. Just at this point, there is a sharp increase in D_f. But immediately after gelation, D_f still increases sharply and continuously. It means that gelation takes place and extends very rapidly. As a result, there are noticeable changes in structure and size of these chains which represent network copolymers. When the sharp increase of D_f values finishes, region 2 is ended.

The last part of the curve in Figure 12 is region 3. Far beyond the gelation time, no more irregular structures take place in the reaction system and eventually form a glass. The D_f value is relatively stable and there is no rapid change. In this period of time there are some fluctuations of D_f values. It is easy to understand because of the time being needed for reaching the more equilibrate network structure, perhaps restructure and so on.

CONCLUSIONS

From our experimental results we can draw the following conclusions: (1) We have succeeded in the systematic and quantitative characterization of crosslinking copolymerization of styrene-DVB including the first-order law, RLCA mechanism, the divergence of molecular weight, size (R_g, R_h) near t_g, distribution, branching, and so on by means of static and dynamic laser light scattering, LC, GPC, and intrinsic viscosity. (2) The critical exponents of this gelation γ, β, δ, τ, and ν_p have been calculated based on experimental data. (3) We have also demonstrated firmly the fractal behavior for this gelation through small angle X-ray scattering as well as static and dynamic laser light scattering. (4) A novel idea about the existence of three regions on the curve of fractal dimension D_f against reaction time t has been suggested. (5) A fractal geometry methodology for characterization of gelation of copolymer has been provided objectively.

The authors thank Professor Wu Peiqiang, from Peking University, and Professor Dong Baozhong from BEPC NL, for supporting and helping with laser and X-ray scattering experiments, respectively.

REFERENCES

1. W. H. Carothers, *Trans Faraday Soc.,* **32,** 39 (1936).
2. P. J. Flory, *J. Am. Chem. Soc.,* **63,** 3083 (1941).
3. W. H. Stockmayer, *J. Chem. Phys.,* **11,** 45 (1943).
4. W. K. Stockmayer, *J. Chem. Phys.,* **12,** 125 (1944).
5. J. Mikes and K. Dusek, *Macromolecules,* **15,** 93 (1982).
6. H. Tobita and A. E. Hamielec, *Makromol. Chem., Macromol. Symp.,* **20/21,** 501 (1988).
7. H. Tobita and A. E. Hamielec, *Macromolecules,* **22,** 3098 (1989).
8. R. Bansil, H. J. Hermann, and D. Stauffer, *Macromolecules,* **17,** 998 (1984).
9. T. Vicsek, *Fractal Scientific, Growth Phenomena,* World Singapore-New Jersey-London-Hong Kong, 1989.
10. T. H. Zheng, Ms. Thesis, Nankai University, 1993.
11. G. Hild and P. Rempp, *Pure and Appl. Chem.,* **53,** 1541 (1981).
12. P. J. Flory, *Principles of Polymer Chemistry,* Cornell, London, 1953.
13. J. P. Munch and M. Ankrim, *Macromolecules,* **17,** 110 (1984).
14. E. V. Patton, J. A. Wesson, M. Rubinstein, J. C. Wilson, and L. E. Oppenheimer, *Macromolecules,* **22,** 1946 (1989).
15. J. Zarzycki, *J. of Non-Crystalline Solid,* **95 & 97,** 173 (1987).
16. B. Chu and C. Woo, *Macromolecules,* **6,** 1729 (1988).
17. W. D. Brown and R. C. Ball, *J. Phys.,* **A18,** 517 (1985).
18. R. Jullien, *Phys. Rev. Lett.,* **55,** 1697 (1985).
19. R. Jullien, *J. Phys.,* **A19,** 2129 (1986).
20. D. A. Weitz, J. L. Huang, and M. Y. Lin, *Phys. Rev. Lett.,* **54,** 1416 (1985).
21. B. Jullien and R. Botet, *Aggregation and Fractal Aggregates,* World Scientific, Singapore-New Jersey-London-Hong Kong, 1987.